# Change in Electronic Structure of Polyenes Due to Interaction with Polyacenes and with Graphitic Strips

**I. A. Howard,*,† D. J. Klein,‡ N. H. March,†,§ C. Van Alsenoy,|| S. Suhai,⊥ Z. Jánosvalfi,⊥,# and Á. Nagy#**

*Department of Physics, University of Antwerp, Groenenborgerlaan 171, B-2020 Antwerp, Belgium, Department of Marine Sciences, Texas A&M University at Galveston, Galveston, Texas 77553, Oxford University, Oxford, England, Department of Chemistry, University of Antwerp, Universiteitsplein 1, B-2610 Antwerp, Belgium, Deutsches Krebsforschungszentrum (DKFZ), Molekulare Biophysik, D-60120 Heidelberg, Germany, and Department of Theoretical Physics, University of Debrecen, H-4010 Debrecen, Hungary*

*Received: January 28, 2004; In Final Form: May 17, 2004*

Hartree−Fock calculations are first presented when a polyene is brought down parallel to the plane of some polyacenes and also, for one case, in a perpendicular orientation. Attention is given to the variation of (a) bond lengths and (b) the HOMO−LUMO energy gap. Following these numerical investigations on finite systems, some tight-binding models (Hückel-like) are worked out to illustrate the effects of different environments on the $\pi$-electron assembly in polyenes. Again the focal points are whether bond alternation is enhanced, or suppressed, and the consequences for the HOMO−LUMO energy gap. Some analytic progress proves possible for an infinite polyene chain interacting with (a) an infinite polyacene and (b) an infinite polyphenacene, when a "hopping" energy is used to couple the polyene with its "environment". In the former model (a), with no HOMO−LUMO gap in the isolated infinite polyacene, a $\pi$−electron polyene gap is opened up. In model (b), a similar variation of the energy gap is found. For future studies, reference is finally made to experiments on the (polyene) chromophore in the retinal protein bacteriorhodopsin. The observed red shift needs mechanisms additional to those considered in the present study, and some suggestions are made here.

## I. Background

In an earlier study in this journal, electronic structure theory was employed to study atomic defects embedded in graphitic fragments.[1] The present work is complementary in that we here bring chemical bonds, in the form of polyenes, from large distances where we can speak of physisorption in materials science parlance, to separations such that the polyene charge distribution overlaps with that in the graphitic-type fragments again considered: this is the chemisorption regime. In principle, experiments related to such physisorption and chemisorption could be carried out for polyene bonds outside a graphene layer, but we are not presently aware of experimental data from such laboratory studies.

The outline of the present paper is as follows. In section II, Hartree−Fock calculations are presented for small polyenes approaching some polyacenes. In particular, anthracene and tetracene have been considered. As well as bringing the polyene near the plane of the polyacene in a parallel configuration, an end-on or perpendicular orientation is also considered in section II. Our focus here will be (a) the change in polyene bond lengths with distance from the polyacene and (b) the modification of the HOMO−LUMO energy gap brought about by "chemisorption" of the polyene on some polyacenes. Section III then treats infinite polyene chains in interaction with (a) an infinite polyacene and (b) an infinite polyphenacene. Here a tight-binding, or Hückel-like, model is adopted. Section IV constitutes a summary, plus some suggestions for future work, including a study of additional mechanisms which will have to be incorporated for an understanding of the red shift found experimentally on the polyene chromophore in the retinal protein bacteriorhodopsin.

## II. Finite Polyenes in Interaction with Some Polyacenes: Hartree−Fock Studies

Hartree−Fock level geometry optimization calculations, using the Gaussian 98 program package,[2] have been carried out on a number of $(CH)_{2n}H_2$ ($n = 3-7$) polyene segments, in cis and trans configurations, interacting with anthracene and tetracene. The 6-31G* basis has been uniformly used. As starting point, we show in Figure 1a the optimized geometry of *cis*-$(CH)_{10}H_2$ and in Figure 1b that of *trans*-$(CH)_{10}H_2$. The corresponding HOMO−LUMO energy gap at this level of calculation is 9.58 eV for *cis*-$(CH)_{10}H_2$ and 9.30 eV for *trans*-$(CH)_{10}H_2$. (It is well-known that a disadvantage of the HF approximation for such systems is that the HOMO−LUMO gap is considerably overestimated.) Increase in conjugation length results in a decrease in the gap; comparable optimizations of *cis*-$(CH)_nH_2$ for $n = 6$ and 14 show variation of the HOMO−LUMO gap from 10.96 eV for $n = 6$ to 8.96 eV for $n = 14$. Geometries of anthracene and tetracene were also optimized at the same level. A referee has raised the possible relevance of correlation with respect to geometry optimization. Inclusion of correlation will produce small changes in the HF geometries. For *cis*-$(CH)_{10}H_2$,

* To whom correspondence should be addressed.
† Department of Physics, University of Antwerp.
‡ Texas A&M University at Galveston.
§ Oxford University.
|| Department of Chemistry, University of Antwerp.
⊥ Deutsches Krebsforschungszentrum (DKFZ).
# University of Debrecen.

10.1021/jp040079k CCC: $27.50 
Published on Web 09/03/2004

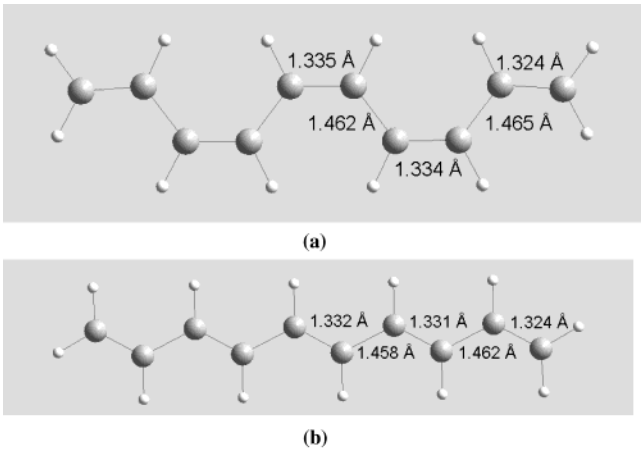


**Figure 1.** Results of Hartree−Fock calculations[2] with the 6-31G* basis, giving the optimized geometries of (a) *cis*-$(CH)_{10}H_2$ and (b) *trans*-$(CH)_{10}H_2$. Note that the bond lengths obtained in (a) and (b) differ only in the third decimal place.

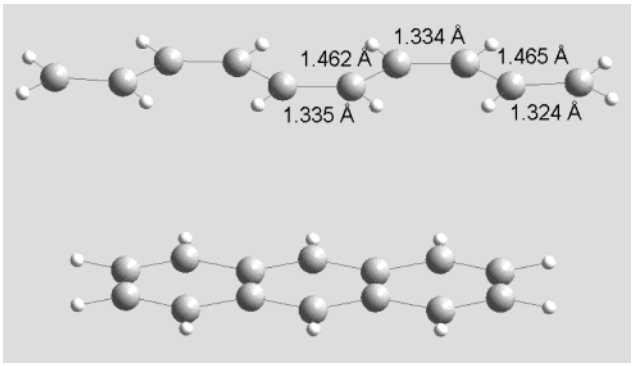


**Figure 2.** Geometry resulting from an unconstrained optimization for *cis*-$(CH)_{10}H_2$ parallel to anthracene, with an initial perpendicular distance of 3 Å; from Hartree−Fock calculations as detailed in Figure 1 above.

for example, an unconstrained second-order Møller−Plesset (MP2)-level geometry optimization results in bond lengths changed by only 1−2% of the HF bond lengths.

We have next considered *cis*- and *trans*-type polyene segments in interaction with anthracene in a parallel configuration. Figure 2 shows the geometry resulting from an unconstrained optimization for *cis*-$(CH)_{10}H_2$ parallel to anthracene, starting from an initial perpendicular distance of 3 Å between the polyene and anthracene. The resulting optimal perpendicular distance between the polyene chain and anthracene is ∼4.4 Å; the anthracene molecule remains planar to within 0.5°, whereas the polyene shows a slight upward curvature but remains planar to within 3°. Analysis of the resulting molecular orbitals shows that the HOMO−LUMO gap for orbitals localized primarily on the polyene chain is 9.59 eV; thus, the interaction has virtually no effect on the gap. In contrast, when we consider a *trans*-$(CH)_8H_2$ segment parallel to anthracene, starting now from an initial perpendicular distance of 2 Å between the polyene and anthracene, we find a very different minimum, as shown in Figure 3. The polyene and anthracene are now severely distorted, with bonding at the ends of the chain that is nearly $sp^3$ in character. Bond alternation in the polyene is increased on the whole, which leads to an increase in the HOMO−LUMO gap for the polyene-associated orbitals, from 9.92 eV for the isolated polyene to 10.71 eV. Turning to the end-on (or perpendicular) configuration for chemisorption of polyene on polyacene, the optimized geometry of *cis*-$(CH)_6H_2$ in interaction

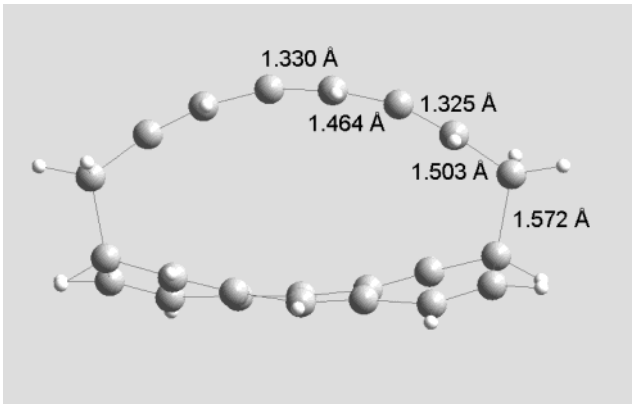


**Figure 3.** *trans*-$(CH)_8H_2$ segment parallel to anthracene, starting from an initial perpendicular distance of 2 Å.

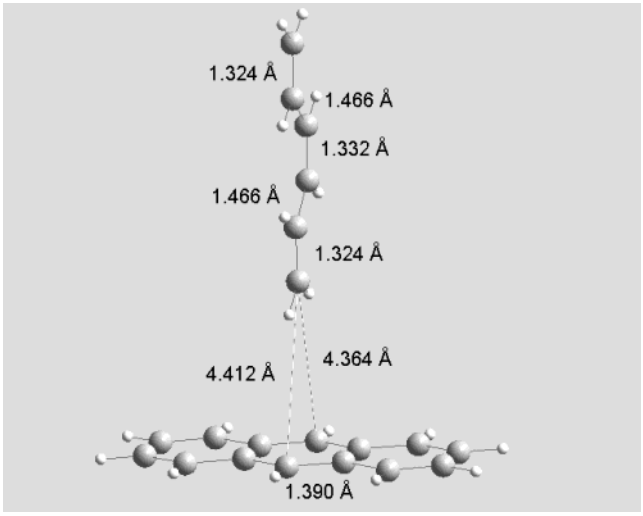


**Figure 4.** Optimized geometry of *cis*-$(CH)_6H_2$ perpendicular to anthracene. Note, by comparison with Figure 1a, the tiny bond length differences on the polyene caused by interaction with anthracene.

with anthracene is shown in Figure 4. Again, as in free space, the polyene bond lengths are 1.33 and 1.47 Å and are little influenced by the proximity of anthracene. The near-neighbor C−C distance shown in this "chemisorption" picture is ∼4.4 Å; the difference of 0.05 Å between the two labeled distances reflects the slight transverse bending of the polyene, even in isolation. The HOMO−LUMO gap associated with the polyene orbitals is now 10.96 eV, as in the isolated polyene.

Finally, we have considered the absorption of *cis*-$(CH)_{10}H_2$ on tetracene, starting from a parallel configuration with a 2 Å vertical separation. The two molecules were given a very slight (∼.01 Å) relative transverse shift, so that their symmetry planes did not exactly coincide. What is remarkable to us is the quite different type of interaction, apparent from Figure 5, than the weak physisorption type behavior shown in Figure 4 for anthracene. The polyene-associated HOMO−LUMO gap is now 10.0 eV. There is now a genuine chemisorption and a really strong coupling between the polyene and the four-ring polyacene. Nevertheless, despite the quite different behavior in Figure 5 compared with that in Figure 4, it remains true that in neither case is there a reduction of the polyene HOMO−LUMO gap.

Thus, at this level of calculation, interaction between a finite polyene and an anthracene or tetracene substrate does not, in any case considered, act to reduce the polyene HOMO−LUMO gap.

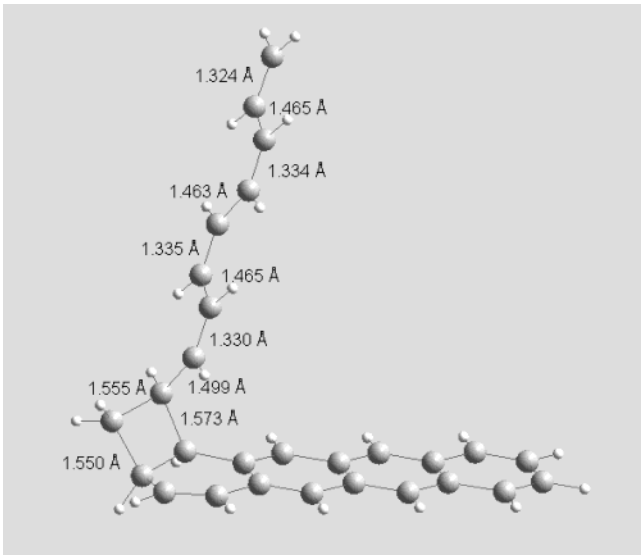


**Figure 5.** Absorption of *cis*-$(CH)_{10}H_2$ on tetracene, initially parallel with 2 Å separation. In marked contrast to Figure 4, the optimized geometry of *cis*-$(CH)_{10}H_2$ on tetracene shows a much stronger "chemisorption" interaction than the "physisorption" type of weak coupling shown in Figure 4 for anthracene.

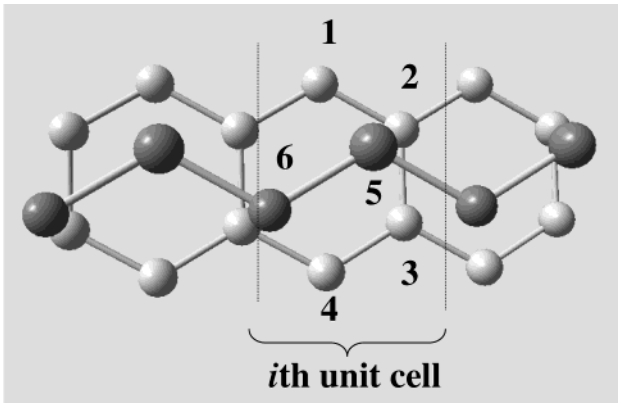


**Figure 6.** Considered arrangement of a *trans*-polyene chain sitting (at a nonbonded distance) above an underlying polyacene chain of hexagons. The alternating single and double bonds are reflected in an alternating bond length (and electron-hopping matrix element). A unit cell is shown, with the site-numbering employed.

### III. Environmental Effect of Polyacene on Electronic Structure of Polyene

Below, we shall study by a tight-binding (TB) model the effect on the electronic structure of the polyene of a polyacene strip. We shall model the effects we wish to study by treating both the polyene and the polyacene as infinite in length. The merit of taking this limit is that the electronic states of the resulting $\pi-$electron assembly can be neatly classified by a **k** vector along the chains. As chemically relevant, we note here that, although we study again an infinite strip, only six- or seven-ring systems have been synthesized to date in polyacenes; these become intensely colored and are highly reactive. We do not expect our main conclusions to change if the infinite strip, which allows techniques of energy band theory to be utilized, is replaced by finite polyacenes with $\sim$6 rings.

The arrangement of the polyene over the polyacene is as in Figure 6, with the numbering of the $\pi$ centers within a unit cell as indicated. As a referee has pointed out, commensurability (or the absence thereof) between the two lattices is a somewhat difficult issue. We argue here that the qualitative predictions of the present model calculations should not seriously depend on the exact constructions of the unit cells. The $\pi$-electron Hamiltonian may be represented as a sum of terms $h_i$ for interactions within the unit cell $i$ and terms $v_{ii+1}$ and $v_{i+1i} \equiv v_{i,i+1}^{\dagger}$ for interactions between sites in unit cells $i$ and $i+1$. Then the simple tight-binding $\pi$-electron Hamiltonian may be expressed as

$$H = \sum_{i}^{\text{unit cells}} \{h_i + v_{i,i+1} + v_{i+1,i}\} \tag{1}$$

These interaction operators may then be expressed as

$$h_i = t\{X_{ii}^{12} + X_{ii}^{21} + X_{ii}^{23} + X_{ii}^{32} + X_{ii}^{34} + X_{ii}^{43}\} + t(1+\Delta)\{X_{ii}^{56} + X_{ii}^{65}\} + t'\{X_{ii}^{25} + X_{ii}^{52}\}$$

$$v_{ii+1} = t\{X_{ii+1}^{21} + X_{ii+1}^{34}\} + t(1-\Delta)X_{ii+1}^{56} + t'X_{ii+1}^{36} \tag{2}$$

where the $t$, $t'$, and $\Delta$ are parameters and the $X_{ij}^{ab}$ are operators transferring an electron from site $b$ of unit cell $j$ to site $a$ of unit cell $i$. That is

$$X_{ij}^{ab} \equiv c_{ia\uparrow}c_{jb\uparrow} + c_{ia\downarrow}c_{jb\downarrow} \tag{3}$$

where $c_{ia\sigma}^{+}$ and $c_{ia\sigma}$ are Fermion creation and annihilation operators for a spin$-\sigma$ orbital on site $a$ of unit cell $i$. Here we have allowed (with $\Delta \neq 0$) for bond alternation in the polyene which is the focus of our study, but we have ignored bond localization in the polyacene substrate, where this localization should be less pronounced than in the polyene. A physically reasonable value for $\Delta$ is $\approx$0.1, which corresponds to a considerably reduced HOMO$-$LUMO gap compared with HF. The gaps from HF calculations on short segments are considerably larger than those we use in our TB calculations on extended chains, for several reasons. The gap will be of course heavily influenced by correlation. (The gap in the *cis*-$(CH)_{10}H_2$ segment mentioned above is reduced by $\sim$15% in going from HF to MP2 level.) The gap reduction in polyacetylene due to quasiparticle effects will be even larger, about 50$-$60%. The value used here in our TB calculations for the bond-alternation parameter $\Delta$ reflects standard gap values for the infinite polyacetylene chain; this value thus results from a perspective that essentially includes the effects mentioned above. We stress, as prompted again by constructive comments from a referee, that, although in our model calculations the absolute values of the gap may be different at HF, MP2, or TB levels, what matters are the relative values, and observed tendencies, within one model.

The basic electron-hopping parameter $t$ is taken to be the same ($\approx -3$ eV) for both the polyene and polyacene. The parameter $t'$ couples the two chains in a simple manner, with $t'$ varying with separation between the polyene and polyacene chains. As a typical value for somewhat weakly interacting chains, we might take $t' = t/5$, though for stronger couplings (i.e., closer contact) we might take $t'$ up to $\approx t/2$.

The solution of the Hamiltonian is readily facilitated through a transformation to wave-vector space. That is, the Hamiltonian can be represented in terms of Bloch-type orbitals

$$\phi_{ka} \equiv \frac{1}{\sqrt{N}} \sum_{m=1}^{N} \exp(ikm)\chi_{ma} \tag{4}$$

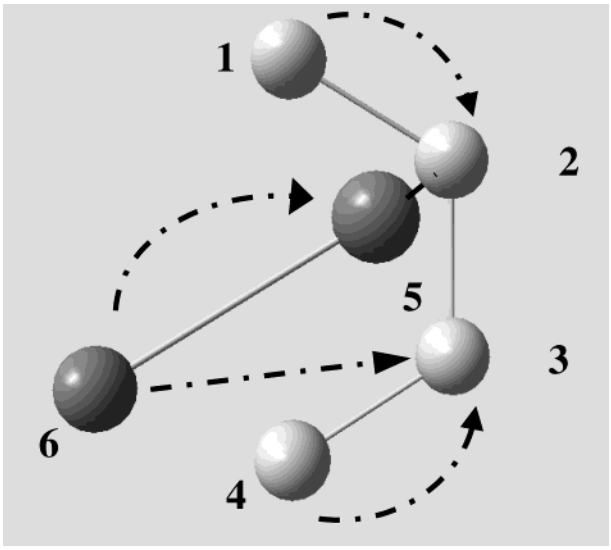


**Figure 7.** Condensed representations for the polyene/polyacene chain. All of the unit cells may be viewed atop one another, with the intercell interactions as indicated by dotted directed lines. Thus, for example, referring back to Figure 6, atom 5 in one cell along the polyene chain interacts with atom 6 in the next cell, and atom 2 in one cell along the polyacene chain interacts with atom 1 in the adjacent cell.

where $\chi_{ma}$ is an atomic orbital for site $a$ of cell $m$, $N$ is the length of the chains (as measured by the number of unit cells), and $k$ is a (one-dimensional) wavevector $2\pi n_k/N$, $n_k = 1, 2, ..., N$. With cyclic boundary conditions, the one-electron representation of $H$ then breaks up into blocks of unit-cell sizes (i.e., 6 by 6):

$$[H^{(k)}] = \begin{pmatrix} 0 & t(1+z) & 0 & 0 & 0 & 0 \\ t(1+\bar{z}) & 0 & t & 0 & t' & 0 \\ 0 & t & 0 & t(1+\bar{z}) & 0 & t'\bar{z} \\ 0 & 0 & t(1+z) & 0 & 0 & 0 \\ 0 & t' & 0 & 0 & 0 & t_+ + t_-\bar{z} \\ 0 & 0 & t'z & 0 & t_+ + t_-z & 0 \end{pmatrix} \quad (5)$$

where $z \equiv \exp(ik)$, $t_+ \equiv t(1 + \Delta)$, and $t_- \equiv t(1 - \Delta)$. In fact, one may readily discern the structure of these blocks from the condensed pictorial representation of the interactions seen in Figure 7.

These may be diagonalized at a sufficient number of $k$ values to clearly display the form of the bands, as are shown in Figure 8, parts a−c. In Figure 8a the bands with no interaction ($t' = 0$) between the polyene and polyacene are shown, and in parts b and c the results with increasing strengths of interaction ($t' = t/5$ and $2t/5$) are shown. Note that the unit cell for the polyene + polyacene system must contain one repeat unit of the polyacene and, thus, in our construction necessarily contains two C's along the polyacetylene backbone. The unit cell in $k$−space runs from zero to $2\pi$, with the polyene gap opening up at $k = \pi$. Evidently in this case, the polyene bands are shifted apart as the interaction $t'$ is turned on. That is, a blue shift for HOMO−LUMO transitions is predicted.

For the polyphenacene/polyene case, we consider the polyene chain in a cisoid form to be located over and parallel to the polyphenacene chain as indicated in Figure 9. A glide translation carries a unit cell of six $\pi$−centers to adjacent unit cells, and the sites within each unit cell are numbered as in Figure 9a.

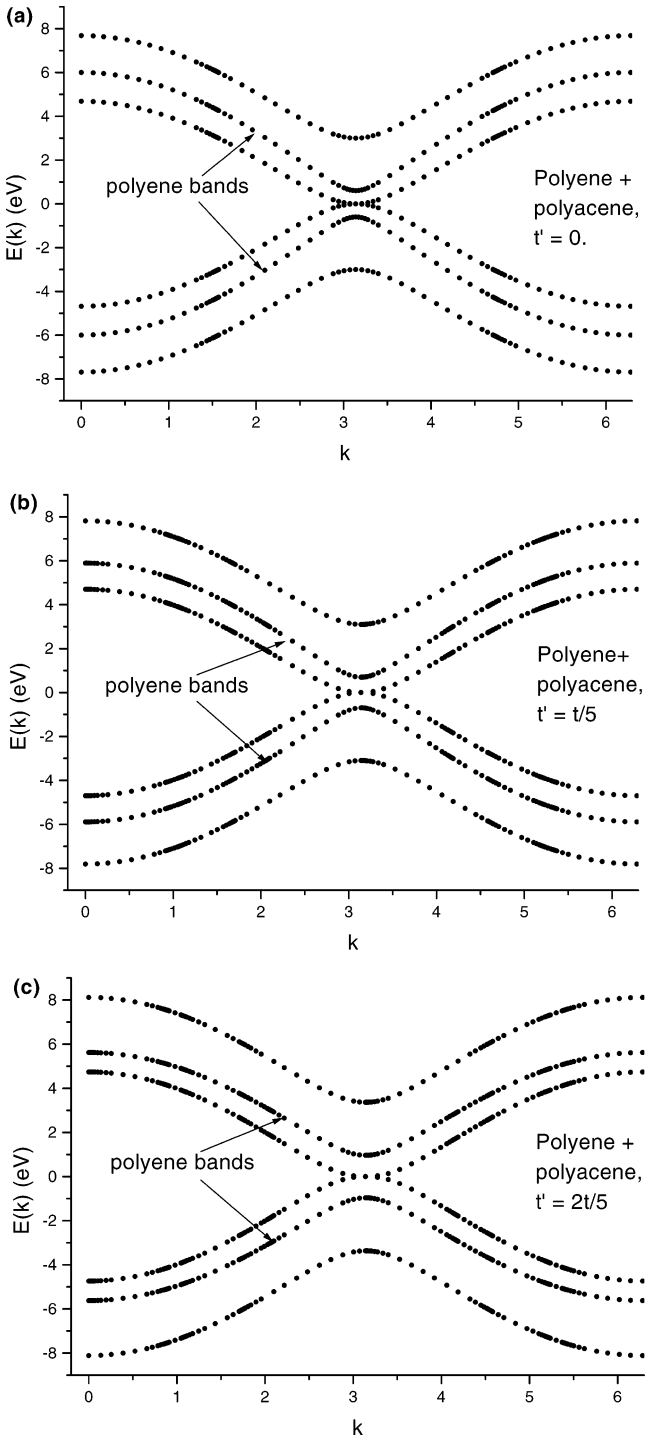


**Figure 8.** Calculated band structure for the polyene + polyacene system with (a) $t' = 0$, (b) $t' = t/5$, (c) $t' = 2t/5$.

Then the simple tight-binding $\pi$-electron Hamiltonian may again be expressed in terms of $h_i$ and $v_{i,i+1}$, where $h_i$ consists of all of the interactions within a unit cell $i$, and $v_{i,i+1}$ and $v_{i+1,i} \equiv v_{i,i+1}^{\dagger}$ consist of the interactions between adjacent cells $i$ and $i + 1$. These interaction operators may in this case be expressed as

$$h_i = t\{X_{ii}^{12} + X_{ii}^{21} + X_{ii}^{34} + X_{ii}^{43}\} + t(1+\Delta)\{X_{ii}^{56} + X_{ii}^{65}\}$$

$$v_{i,i+1} = t\{X_{ii+1}^{23} + X_{ii+1}^{21} + X_{ii+1}^{41}\} + t(1-\Delta)X_{ii+1}^{65} + t'\{X_{ii+1}^{25} + X_{ii+1}^{61}\} \quad (6)$$

We have again allowed (with $\Delta \neq 0$) for bond alternation in the polyene which is the focus of our study, but we have ignored

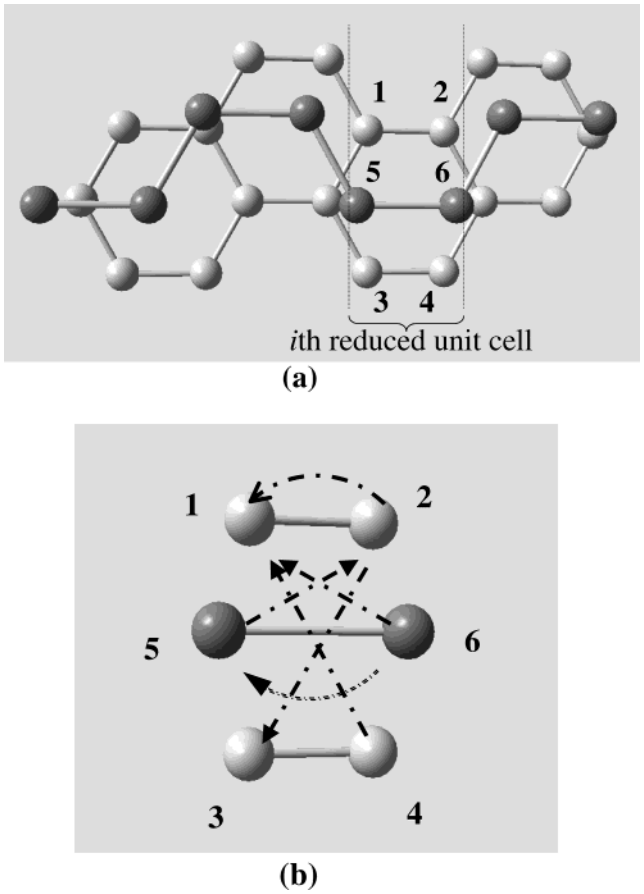


**Figure 9.** Condensed representations for the *cis*-polyene/polyphenacene system. In (a) a reduced unit cell is shown, with the site numbering employed, and the vertical dashed lines marking the boundaries between unit cells. In (b) all unit cells may be viewed as superimposed with corresponding sites sitting atop one another and the intercell interactions now indicated by directed dotted lines, as for the polyene/polyacene system in Figure 7.

bond localization in the polyphenacene substrate, where this localization should be less pronounced than in the polyene. As before we take $\Delta \approx 0.1$, and the basic electron-hopping parameter $t$ is taken to be the same ($\approx -3$ eV) for both the polyene and polyphenacene.

Again, we transform to wave-vector space. Now, with cyclic boundary conditions, the one-electron representation of $H$ breaks up into blocks of unit-cell sizes (i.e., 6 by 6):

$$[H^{(k)}] = \begin{pmatrix} 0 & t(1+\bar{z}) & 0 & t\bar{z} & 0 & t'\bar{z} \\ t(1+z) & 0 & tz & 0 & t'z & 0 \\ 0 & t\bar{z} & 0 & t & 0 & 0 \\ tz & 0 & t & 0 & 0 & 0 \\ 0 & t'\bar{z} & 0 & 0 & 0 & t_+ + t_-\bar{z} \\ t'z & 0 & 0 & 0 & t_+ + t_-z & 0 \end{pmatrix} \quad (7)$$

where, as before, $z \equiv \exp(ik)$, $t_+ \equiv t(1+\Delta)$, and $t_- \equiv t(1-\Delta)$. The condensed pictorial representation of the interactions, as shown in Figure 9b, illustrates the structure of these blocks.

With the blocked representation of eq 7, computations at a representative set of $k$ values are readily made to reveal the structure of electronic bands. The results are exhibited in Figure 10, parts a−c. In Figure 10a, the bands for the noninteracting ($t' = 0$) case are exhibited, with the innermost band (i.e., that nearer $\epsilon = 0$) being that for the polyene. In Figure 10, parts b and c, the interaction strength is increased from $t' = t/5$ to $t' = 2t/5$.

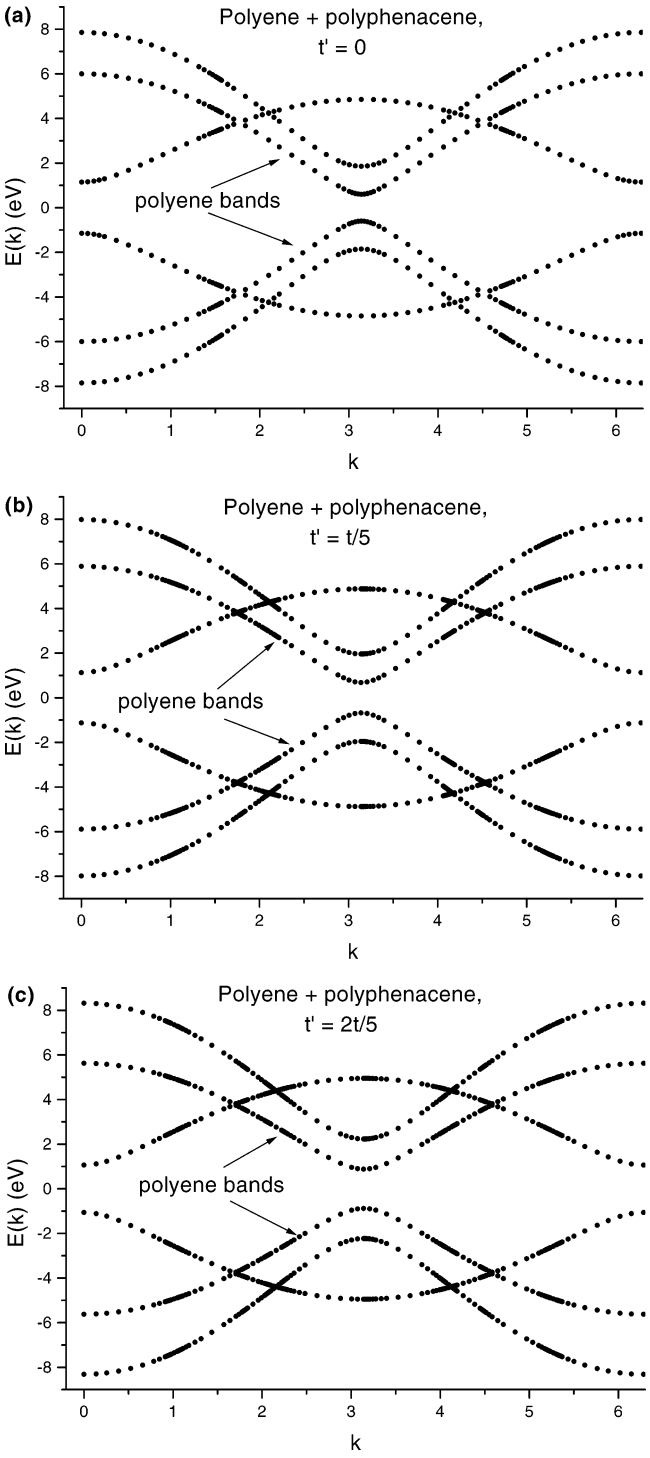


**Figure 10.** Calculated band structure for the polyene + polyphenacene system with (a) $t' = 0$, (b) $t' = t/5$, (c) $t' = 2t/5$.

## IV. Discussion and Future Directions

We have made here a study of polyenes interacting with various types of graphitic fragments. Thus, in section II, we have been concerned with finite hydrocarbon clusters, and in particular with polyacetylene segments interacting first with anthracene and second with tetracene. To us, the most remarkable finding of the present Hartree−Fock study is the strong coupling between tetracene and the polyene, as evidenced in Figure 5. This is seen to be qualitatively different from the

modest "physisorption" type of interaction of a similar polyene with anthracene in the perpendicular configuration.

The remaining part of the present study has dealt with two types of, now infinite, graphitic strips interacting with polyacetylene. The calculations presented, although carried out within a tight-binding framework, have the merit that much progress proves possible at an analytical level. The same conclusion results, however: namely, that interaction of the polyenes considered with finite, or infinite, planar hydrocarbon strips leaves the HOMO−LUMO gap either increased or, for the polyene in perpendicular configuration on anthracene, results in practically no change in the gap.

However, having said that, it is relevant in this discussion to contrast different features of the infinite strips of polyacene and polyphenacene. In gross terms, although an isolated strip of polyphenacene has an energy gap in the $\pi$−electron states at the HOMO (Fermi) level and, therefore, in condensed matter parlance is akin to an "insulator", the polyacene strip has a high density of electronic states near the Fermi energy. Since reference was made already in section I above to a graphene layer, where $\pi$-bands touch at the Fermi level, it is grossly true to say that polyphenacene is "more like graphene" (a single graphene layer having semimetallic character) than polyacene, the latter having a "spike" in the density of states near the Fermi level.

As to future studies, for which the present modeling of proximity effects on the HOMO−LUMO energy separation in a polyene chain may have some relevance, we want to stress the availability of experiments on the (polyene) chromophore in the retinal protein bacteriorhodopsin. The observed red shift, we want to emphasize in concluding this discussion, will plainly require the incorporation of mechanisms in proximity "perturbations" additional to those considered in the present modeling. A relevant reference is the very recent study of Sakurai et al.[3] One "hint" from the present study is that very asymmetric perturbations, as in Figures 4 and 5 above, leave the HOMO−LUMO gap at least little changed in the polyene. As treated by earlier authors, such end effects can give rise to localized or evanescent states, and their effect in perturbing the optical properties of an initially "free space" polyene chain will be of interest for future studies. There may also be effects due to electronegativity differences that are also relevant perturbations on the polyene chromophore in bacteriorhodopsin. As a final comment, it seems clear that dispersion interactions will play a role in the interaction between planar conjugated systems such as those studied here. Hartree−Fock, and also DFT, calculations, as mentioned by Elstner et al.,[4] are both deficient in this regard, and further work is called for in this area.

**Acknowledgment.** I.A.H. acknowledges support from the IWT-Flemish region under Grant IWT-161. D.J.K. acknowledges the support of the Welch Foundation of Houston, TX. Part of this work was supported by the Ministry of the Flemish community under contract BIL01/72 in the framework of the bilateral scientific cooperation between Belgium and Hungary and by the University of Antwerp under Project GOA-BOF-UA nr. 23, and by the Bilateral Scientific and Technological Cooperation between Hungary and Flanders (project No. B-2/01). We also thank the University of Antwerp for support under Grant BOF UA/SFO UIA2002.

## References and Notes

(1) Peeters, A.; Van Alsenoy, C.; March, N. H.; Klein, D. J.; Van Doren, V. E. *J. Phys. Chem. B* **2001**, *105*, 10546.

(2) Frisch, M. J.; Trucks, G. W.; Schlegel, H. B.; Scuseria, G. E.; Robb, M. A.; Cheeseman, J. R.; Zakrzewski, V. G.; Montgomery, J. A., Jr.; Stratmann, R. E.; Burant, J. C.; Dapprich, S.; Millam, J. M.; Daniels, A. D.; Kudin, K. N.; Strain, M. C.; Farkas, O.; Tomasi, J.; Barone, V.; Cossi, M.; Cammi, R.; Mennucci, B.; Pomelli, C.; Adamo, C.; Clifford, S.; Ochterski, J.; Petersson, G. A.; Ayala, P. Y.; Cui, Q.; Morokuma, K.; Malick, D. K.; Rabuck, A. D.; Raghavachari, K.; Foresman, J. B.; Cioslowski, J.; Ortiz, J. V.; Stefanov, B. B.; Liu, G.; Liashenko, A.; Piskorz, P.; Komaromi, I.; Gomperts, R.; Martin, R. L.; Fox, D. J.; Keith, T.; Al-Laham, M. A.; Peng, C. Y.; Nanayakkara, A.; Gonzalez, C.; Challacombe, M.; Gill, P. M. W.; Johnson, B. G.; Chen, W.; Wong, M. W.; Andres, J. L.; Head-Gordon, M.; Replogle, E. S.; Pople, J. A. *Gaussian 98*, revision A.7; Gaussian, Inc.: Pittsburgh, PA, 1998.

(3) Sakurai, M.; Sakata, K.; Saito, S.; Nakajima, S.; Inoue, Y. *J. Am. Chem. Soc.* **2003**, *125*, 3108.

(4) Elstner, M.; Hobza, P.; Frauenheim, T.; Suhai, S.; Kaxiras, E. *J. Chem. Phys.* **2001**, *114*, 5149. See also: Reha, D.; Kabelac, M.; Ryjacek, F.; Sponer, J.; Sponer, J. E.; Elstner, M.; Suhai, S.; Hobza, P. *J. Am. Chem. Soc.* **2002**, *124*, 3366.